



Published in final edited form as:

Dev Biol. 2007 October 1; 310(1): 71–84. doi:10.1016/j.ydbio.2007.07.027.

Zebrafish *bmp4* functions during late gastrulation to specify ventroposterior cell fates

Heather L. Stickney¹, Yoshiyuki Imai¹, Bruce Draper², Cecilia Moens², and William S. Talbot¹

¹ Stanford University School of Medicine, Department of Developmental Biology, Stanford, CA 94305, USA

² Fred Hutchinson Cancer Research Center, HHMI and Division of Basic Science, Seattle, WA 98115, USA

Abstract

Bone morphogenetic proteins (BMPs) are key mediators of dorsoventral patterning in vertebrates and are required for the induction of ventral fates in fish and frogs. A widely accepted model of dorsoventral patterning postulates that a morphogenetic BMP activity gradient patterns cell fates along the dorsoventral axis. Recent work in zebrafish suggests that the role of BMP signaling changes over time, with BMPs required for global dorsoventral patterning during early gastrulation and for tail patterning during late gastrulation and early somitogenesis. Key questions remain about the late phase, including which BMP ligands are required and how the functions of BMPs differ during the early and late gastrula stages. In a screen for dominant enhancers of mutations in the homeobox genes *vox* and *vent*, which function in parallel to *bmp* signaling, we identified an insertion mutation in *bmp4*. We then performed a reverse genetic screen to isolate a null allele of *bmp4*. We report the characterization of these two alleles and demonstrate that BMP4 is required during the later phase of BMP signaling for the specification of ventroposterior cell fates. Our results indicate that different *bmp* genes are essential at different stages. In addition, we present genetic evidence supporting a role for a morphogenetic BMP gradient in establishing mesodermal fates during the later phase of BMP signaling.

Keywords

BMP4; BMP2b; BMP7; dorsoventral patterning; zebrafish; Vox; Vent

INTRODUCTION

The dorsoventral axis of the vertebrate embryo is patterned by a conserved mechanism involving β -catenin, members of the bone morphogenetic protein (BMP) family, and BMP antagonists. In zebrafish, genes required for ventral specification, including *bmp2b*, *bmp7* and the homeobox gene *vox*, are uniformly expressed throughout the blastula shortly after the onset of zygotic transcription at the midblastula transition (MBT) (Kawahara et al., 2000a; Nikaido et al., 1997; Schmid et al., 2000). The *bmps* activate the expression of ventral genes, such as the erythroid lineage marker *gata1* and the *bmps* themselves, while *vox* and its homologs *vent* and *ved* function to repress the expression of dorsal-specific genes like the *bmp* antagonist *chordin* and the homeobox gene *gooseoid* (Imai et al., 2001; Shimizu et al., 2002). Zebrafish

Publisher's Disclaimer: This is a PDF file of an unedited manuscript that has been accepted for publication. As a service to our customers we are providing this early version of the manuscript. The manuscript will undergo copyediting, typesetting, and review of the resulting proof before it is published in its final citable form. Please note that during the production process errors may be discovered which could affect the content, and all legal disclaimers that apply to the journal pertain.

embryos lacking BMP2b (*swirl*), BMP7 (*snailhouse*), Vox and Vent (*Df^{st7}* in the TL strain) or Vox, Vent and Ved (morphants in the AB strain) activity are severely dorsalized, with expanded trunk somitic fates, reduced blood, vasculature, and pronephros fates, and loss of tail tissue (Dick et al., 2000; Imai et al., 2001; Kishimoto et al., 1997; Nguyen et al., 1998; Schmid et al., 2000; Shimizu et al., 2002). Recent work suggests that the initiation of *bmp2b* expression is under the control of a maternal pathway involving Pou2, the TGF β protein Radar and Smad5, a downstream component of the Bmp signaling pathway (Kramer et al., 2002; Reim and Brand, 2006; Sidi et al., 2003). The maternal factors required for the initiation of *bmp7* and *vox* expression are unknown.

Dorsal fate is established through the asymmetric action of maternal β -catenin protein, which accumulates in the nuclei of blastomeres in a small marginal domain (reviewed in Hibi et al., 2002). Following MBT, maternal β -catenin, in concert with the HMG-box protein Tcf/Lef, activates the expression of the homeobox gene *bozozok*. *Boz*, which is required for the development of dorsal structures, functions to repress the expression of the *bmps* and *vox* (Fekany et al., 1999; Imai et al., 2001; Koos and Ho, 1999; Ryu et al., 2001; Shimizu et al., 2002). By late blastula, the presumptive organizer region expresses little *bmp* and *vox* mRNA, allowing for the activation of *chordin* and *gooseoid* and other dorsal-specific genes in this region.

According to a widely accepted model, this initial phase of dorsoventral patterning is followed by a second phase in which a morphogenetic BMP activity gradient is generated through the interplay between BMP antagonists and agonists (reviewed in Schier and Talbot, 2005). In this model, high levels of BMP activity specify ventral fates, lower levels induce more lateral fates and absence of BMP activity leads to the adoption of dorsal fates. Proper regulation of BMP activity is crucial for dorsoventral patterning. Mutations in genes that antagonize BMP signaling, such as the BMP antagonist *chordin* (*chordino*) and the *tolloid* antagonist *sizzled* (*ogon*), result in the expansion of ventral tissues at the expense of dorsal (Martyn and Schulte-Merker, 2003; Schulte-Merker et al., 1997; Yabe et al., 2003), while loss of Tolloid (Minifin), BMP1 and Twisted Gastrulation, all of which function as activators of the BMP pathway, causes dorsalized phenotypes (Connors et al., 1999; Jasuja et al., 2006; Little and Mullins, 2004; Muraoka et al., 2006).

The best genetic evidence for a morphogenetic BMP activity gradient comes from the analysis of neural crest in the ectoderm (Nguyen et al., 1998). Neural crest is absent in *swr* (*bmp2b*) mutants, which have a strong reduction in BMP signaling. However, milder reduction of BMP signaling, as in hypomorphic *snh* (*bmp7*) mutants and strong *sbm* (*smad5*) mutants, causes a striking expansion of neural crest. The paradoxical expansion of a fate that requires BMP signaling in mutants with lowered BMP activity is explained, and in fact predicted, by a gradient model. Reducing overall BMP activity results in a shallower BMP gradient, such that more cells along the dorsoventral axis are exposed to BMP activity levels that fall between the upper and lower thresholds for neural crest specification. BMPs may act as morphogens in the mesendoderm as well, but similar evidence of expanded intermediate territories is lacking, leaving open alternative models involving relay signals.

Recently, experiments with a heat-shock inducible dominant-negative BMP receptor have suggested that the role of BMP signaling changes over time (Pyati et al., 2006; Pyati et al., 2005). Reduction of BMP signaling during blastula and early gastrula stages disrupts ventral mesoderm and primary tail formation, whereas reduction of BMP signaling during mid-gastrulation prevents cloaca and ventral tail fin formation. The nature of this temporal change in BMP function is unclear. Indeed, BMPs may have opposite functions in tail development at early and late stages, because loss of BMP in the early gastrula eliminates the tail, while loss of BMP in the late gastrula generates ectopic tail tissue. Furthermore, the endogenous BMP

ligand(s) acting in the later phase has not been identified, and it is unclear whether BMPs continue to function as morphogens in the late gastrula.

The role of zebrafish BMP4 in dorsoventral patterning is unclear. In fish and frogs, overexpression of BMP4 RNA leads to the ventralization of wild-type embryos (Dale et al., 1992; Fainsod et al., 1994; Graff et al., 1994; Neave et al., 1997; Schmidt et al., 1995; Suzuki et al., 1994), and *bmp4* overexpression can rescue *bmp2b* (*swr*) and *bmp7* (*snh*) mutants (Hammerschmidt et al., 1996; Kishimoto et al., 1997; Nguyen et al., 1998; Schmid et al., 2000). Furthermore, zebrafish *bmp4* is expressed in ventral cells during late blastula and gastrula stages, in the right time and place to play a role in the patterning of the dorsoventral axis. However, the expression of *bmp4* is delayed in comparison with the expression of the other two *bmps* (Nikaido et al., 1997), suggesting that it may function at later stages than BMP2b and BMP7. No zebrafish *bmp4* mutants have been identified, impeding the analysis of its function.

We report the isolation and analysis of two alleles of *bmp4*. We have determined that BMP4 serves as an endogenous ligand during the later phase of BMP signaling and is required for proper ventroposterior fate specification. Mutants display disrupted cloacal development, reductions in ventral tail fin and alterations in somite and vasculature patterning in the tail. These results demonstrate that the early and late phases of BMP signaling involve different genes. Furthermore, we provide genetic evidence for a morphogenetic role of BMPs in the patterning of tail mesoderm, demonstrating an expansion of tail mesoderm and blood fates upon intermediate reduction of BMPs.

MATERIALS AND METHODS

Mutagenesis and screening

To introduce mutations in a sensitized background, premeiotic mutagenesis with the chemical mutagen N-nitroso-N-ethylurea (ENU, 3mM) was performed on males homozygous for *vox^{st9}*, a null mutation in the *vox* gene (Imai et al., 2001), for three 1-hour periods following standard protocols (van Eeden et al., 1999). The mutagenized males were crossed to wild-type (TL) females and the progeny raised. To identify fish carrying mutations in genes that interact with *vox* and *vent*, female F1 fish were then mated to males heterozygous for a deletion (*D^{st7}*) on LG13 that removes both *vox* and *vent*. The F2 progeny were scored for strength of dorsalization at 24 hpf using the C1-C5 classification scheme (Mullins et al., 1996). In the absence of an enhancer, 2–14% of the progeny from crosses between *vox^{st9}* females and *D^{st7}* males are variably dorsalized (C1-C4/C5) (Imai et al., 2001). We selected for F1 females that yielded at least two clutches in which the penetrance of dorsalization was greater than 15%.

Linkage analysis of *smad5* alleles

Linkage between *smad5* and *st30*, *st31*, *st32*, and *st33* was analyzed by genotyping dorsalized embryos for polymorphic SSLP or RFLP markers in or near the *smad5* locus.

Mapping of *st37*

st37 was initially localized to LG17 by bulked segregant analysis (reviewed in Postlethwait and Talbot, 1997) on pools of genomic DNA from 20 wild-type and 20 mutant 24hpf embryos from an intercross of two *st37* heterozygotes. Primer sequences for simple sequence length polymorphisms (SSLPs) were obtained from the MGH zebrafish database (<http://zebrafish.mgh.harvard.edu>). Embryonic genomic DNA was prepared as described (Talbot and Schier, 1999). To find RFLP markers for higher resolution mapping, we PCR-

amplified and sequenced ESTs that mapped near *bmp4* on the HS, T51, or LN54 panels (Geisler et al., 1999; Hukriede et al., 2001; Woods et al., 2000) in *st37* heterozygotes.

Southern Blots

Genomic DNA was isolated from pools of 40 *st37/st37*, *st37/+*, and *+/+* embryos at 5dpf with a Qiagen DNeasy kit. 10 ug of the genomic DNA was digested with BstXI, PstI, HpyCHIV, NheI, SmlI, SfcI, MmeI, BspMI, or BssSI (NEB), run on a 1% agarose gel, and then transferred to a charged nylon membrane (Hybond-N+, Amersham Biosciences). Probes were amplified from genomic DNA (5' probe: 5'-CCGCTGATAAATAAGAGACTAAGC-3' and 5'-GCTTTAAGCATAATCTGAAATCACTC-3', 667bp; 3'probe: 5'-ACACCGTGCGCATCTCTT-3' and 5'-GGCTGCTAATATGATTTCCCTGT-3', 579bp) and radioactively labeled with the Rediprime II Random Prime Labelling System (Amersham Biosciences). Unincorporated nucleotides removed with Microspin G-25 columns (Amersham Biosciences). Hybridization of the probes to the nylon membrane was performed with Rapid-hyb buffer (Amersham Biosciences) following the supplied protocol.

Reverse Genetic Screen

To identify a null allele of *bmp4*, we screened genomic DNA from 8256 mutagenized F1 males for nonsense mutations with a yeast-based truncation assay developed by Gould and colleagues (Chen and Gould, 2004; Zan et al., 2003). We PCR-amplified the majority of the *bmp4* coding exons (exon 3 and exon 4) from each mutagenized F1 male with PCR primers designed to allow in frame fusion of the *bmp4* coding region with the *ade2* gene in a universal gap repair vector engineered by Chen and Gould (Chen and Gould, 2004). PCR conditions were as follows: 94°C for 3 min and then 45 cycles of 94°C for 30s, 55°C for 30s, 72°C for 30s, followed by 5 min at 72°C. The amplified *bmp4* coding sequence was then integrated upstream of *ade2* by *in vivo* homologous recombination in yIG397 yeast cells following published protocols (Chen and Gould, 2004). Transformants were plated on synthetic minimal media lacking leucine and supplemented with low adenine (5 micrograms/ml). Cells with functional BMP4-Ade2 fusion proteins produce white colonies, whereas a stop codon in the *bmp4* sequence truncates the fusion protein, leading to loss of Ade2 activity and a red colony. Plates were scored visually. Samples that twice produced >25% red colonies were sequenced. A frozen sperm sample from the F1 carrier of *st72*, which yielded 44% red colonies, was thawed and *in vitro* fertilization performed according to standard protocols.

In total, we performed 29080 individual PCRs followed by the same number of yeast transformation reactions in the course of screening 7965kb of *bmp4* coding sequence from the mutagenized F1 males. Multiple primer pairs were used to amplify exon 4 as inclusion of about 50 bases of coding sequence from the middle of the exon in the PCR amplicon caused all yeast colonies to be red, presumably the result of interference with Ade2 function. In addition, poor quality of some DNA samples forced us to screen the coding exons with multiple smaller PCR amplicons. Of the 29080 samples, 472 (~1.6%) yielded >25% red colonies once; only 26 (<<1%) yielded >25% red colonies twice.

Genotyping of embryos

Genotyping of *vox^{st9}* was performed as previously described (Imai et al., 2001). For *swr^{ta72}*, *snh^{ty68a}*, *sbn^{st30}*, *sbn^{st31}*, *sbn^{st32}*, *st33*, *bmp4^{st37}* and *bmp4^{st72}*, we designed primers that allowed us to genotype embryos by PCR and enzymatic digestion (Supplemental Table 1). PCR was performed as follows: 94°C for 3 min, 35 or 45 cycles of 94°C for 30s, 55°C for 30s, 72°C for 1 min, followed by 5 min at 72°C.

5'RACE, RT-PCR, and TA cloning

Total RNA was isolated from adult ovaries and zebrafish embryos using TRIzol Reagent (Gibco/BRL) according to the manufacturer's instructions. First-strand synthesis was performed according to SuperScript First-Strand Synthesis System for RT-PCR (Invitrogen). cDNA spanning the first, second, third, and fourth exons was amplified with the primers ACACCGTGCGCATCTCTT (RTE1F; 3' of the *st37* insertion) and GCTCTGCGGTGGATATGAGT (RTE4R1) or CGTAGCTGGTCCCACTCTTC (RTE4R2). cDNA from the third and fourth exons was amplified with the forward primer TGGTAATCGAATGCTGATGG (RTE3F) and either RTE4R1 or RTE4R2. PCR was performed as follows: 94°C for 3 min, 35 cycles of 94°C for 30s, 55°C for 30s, 72°C for 1 min, followed by 5 min at 72°C.

To determine the relative abundance of *st37* transcripts, RT-PCRs on RNA from heterozygotes were TA-cloned with the TOPO TA Cloning kit (Invitrogen) according to the manufacturer's instructions. Inserts of individual clones were identified through a BslII RFLP in exon 3.

5'RACE was performed with the 5'RACE BD SMART RACE cDNA Amplification Kit (BD Biosciences Clontech) according to the manufacturer's instructions. Primers utilized included both CAGGACGAGCTCCTCAAGCGAATGTTA (5'RACEE2R) and AGCCGACGCTTTCTTCTCCCTTCCT (5'RACEE3R). We used the suggested touchdown PCR program but increased the number of cycles in the final loop to 30. PCR products were TA-cloned as above and inserts sequenced with the M13 Reverse primer.

Whole-mount in situ hybridization

Probe synthesis and in situ hybridizations were performed following standard protocols. Embryos from *st72/+* and *st37/+* intercrosses were genotyped after in situ hybridization as described (Sirotkin et al., 2000).

RESULTS

Insertion allele of *bmp4* isolated in dominant enhancer screen

To identify novel genes involved in dorsoventral patterning, we conducted a forward genetic screen for dominant enhancers of the redundant dorsal repressors *vox* and *vent*. In a screen of 705 mutagenized genomes, we identified 12 putative enhancers of *vox* and *vent*. Seven proved difficult to map and have not been maintained. Of the remaining five mutations, at least three, and probably four, are new alleles of *smad5*. We have identified *smad5* lesions in *st30*, *st31* and *st32*, while *st33* is tightly linked to the *smad5* locus (Table 1).

The final enhancer identified in the dominant enhancer screen, *st37*, has a C1 phenotype with variable penetrance (range 0–68%, mean 21.4%, n=16048) and expressivity in a cross of two heterozygotes with an otherwise wild-type background. We mapped *st37* to a 5cM interval on linkage group 17 between the simple sequence length polymorphism (SSLP) markers Z9692 and Z11340. A strong candidate gene, *bmp4*, is located within that region (Geisler et al., 1999; Hukriede et al., 2001; Shimoda et al., 1999; Woods et al., 2000). BMP4 has been implicated in dorsoventral patterning in frogs and mice (Dale et al., 1992; Fainsod et al., 1994; Graff et al., 1994; Schmidt et al., 1995; Suzuki et al., 1994; Winnier et al., 1995), and overexpression in zebrafish causes ventralization (Neave et al., 1997).

To date, no zebrafish *bmp4* mutants have been reported. The *bmp4* gene comprises four exons, with the coding sequence contained entirely within the last two exons (Shentu et al., 2003). Although we found no coding change in *bmp4* in *st37* mutants, high resolution mapping with a panel of 7475 meioses localized *st37* to an ~8kb critical interval bounded by two single

nucleotide polymorphisms that flank the first, noncoding exon of *bmp4* (Fig 1A). Southern blots on genomic DNA using probes near the first exon indicated that the *bmp4* locus is rearranged in *st37* mutants and suggested the presence of a large insertion (Supplemental Fig 1A,B). Sequencing of the insert ends demonstrated that the insertion occurs in the 5'UTR of *bmp4*, 47b upstream of the 3' end of exon 1. Comparison of the insert end sequences with sequences from the NCBI nucleotide database (<http://www.ncbi.nlm.nih.gov/>) suggests that the insert is 34.581kb in length and originated from LG8 (Fig 1A, Supplemental Fig 1C). Based on these data, it is clear that the first exon of *bmp4* is disrupted in *st37* mutants.

***st37* mutants have reduced levels of *bmp4* mRNA**

To determine the effect of the *bmp4^{st37}* insertion on the *bmp4* gene, we examined mRNA levels in *bmp4^{st37}* mutants. RT-PCR on total RNA from 50–70% epiboly and 24hpf embryos demonstrated that *bmp4* mRNA is significantly reduced in *bmp4^{st37}* homozygous mutants as compared to wild-type and heterozygous siblings (Fig 1B). The reduction in *bmp4* expression in *st37* homozygous embryos is also evident by in situ hybridization at all stages examined (Fig 1C–F and data not shown). To measure the reduction in mRNA expression from the *bmp4^{st37}* allele, we quantitated the relative levels of wild-type and mutant RNA in cloned RT-PCR products from *bmp4^{st37}* heterozygotes using SNPs to distinguish the alleles. A strong reduction in mutant RNA levels was apparent at both embryonic stages analyzed: in total only 9 out of 342 tested clones were generated from the mutant allele (2.63%, Table 2). Interestingly, a similar analysis performed on RNA from dissected adult ovaries indicated that a significant amount of *bmp4* is generated from the mutant allele in ovaries (Fig. 1B). Moreover, these transcripts have a novel structure, as most mutant *bmp4* RNAs lack the first exon of *bmp4* and instead comprise sequences from the LG8 insertion fused to the remaining exons of *bmp4* (Table 2 and data not shown). The combination of all of these results suggests that *bmp4^{st37}* is not a null allele.

Reverse genetic screen for a null allele of *bmp4*

To identify a null allele of *bmp4*, we searched for nonsense mutations in *bmp4* by screening genomic DNA from a library of mutagenized F1 fish with a yeast-based truncation assay (Chen and Gould, 2004). We screened a total of 7965kb of genomic DNA comprising the majority of the *bmp4* coding region in 8256 ENU-mutagenized F1 fish. We identified one *bmp4* allele, *bmp4^{st72}*, containing a G to T nonsense mutation in the fourth exon of *bmp4* that changes Glu (209) to a stop (Fig 1G). This mutation causes truncation of the BMP4 protein prior to the mature peptide domain (Fig 1H) and is predicted to eliminate all BMP4 function. In support of this, *bmp4* mRNA containing the *st72* lesion has no activity (ventralizing or dorsalizing) in overexpression assays (data not shown).

***bmp4^{st37}* and *bmp4^{st72}* homozygotes and heterozygotes display variable C1 dorsalization**

bmp4^{st37} and *bmp4^{st72}* mutants both display variable C1 dorsalization, ranging from a subtle reduction in tail fin to a more complete loss of tail fin coupled with reductions in caudal tail vasculature and ventral somitic mesoderm (e.g. see Fig 4C–E). In general, the *bmp4^{st37}* allele exhibits weaker dorsalization effects and lower penetrance than the *bmp4^{st72}* allele. In crosses between *bmp4^{st37}* heterozygotes, we have observed a mean of 21.4% dorsalization (n=16048, range 0–68%), always limited to partial loss of tail fin. In contrast, clutches from crosses between *bmp4^{st72}* heterozygotes have a mean of 49.7% dorsalization (n=782, range 8.6–92%) with mutants in some crosses exhibiting severe C1 dorsalization. However, all embryos from crosses between *bmp4^{st37}/bmp4^{st72}* transheterozygotes have similar phenotypes at 24hpf (n=377), so the differences in phenotypic strength may be due to differences in genetic background rather than differences in allelic strength. The two alleles were isolated from different stocks, and it is clear that both the strength and the penetrance of the mutant

phenotypes are strongly dependent on genetic background. For example, a *bmp4^{st72/+}* female mated to an AB male produced a 55% dorsalized clutch (33/60), while only 2% of the offspring of that same female crossed to a TL male were dorsalized (1/59).

Two observations indicate that the *bmp4* mutations have a dominant effect in some genetic backgrounds. First, a greater than expected percentage of dorsalized embryos (*i.e.* >25%) was observed in a subset of crosses between *bmp4* heterozygotes. In addition, there were dorsalized embryos in crosses between *bmp4* heterozygotes and wild-type fish. However, the percentage of homozygotes that were dorsalized was always much higher than the percentage of dorsalized heterozygotes.

bmp4^{st37} and *bmp4^{st72}* mutants are homozygous viable in genetic backgrounds in which the expressivity of the alleles is weak. To determine whether BMP4 is required maternally, we mated homozygous *bmp4^{st72}* adult females to heterozygous males. In some crosses, 90% of heterozygous embryos exhibited a wild-type phenotype (the other 10% displayed a weak C1 phenotype), indicating that there is no strict maternal requirement for BMP4.

Disrupted development of ventral tissues in *bmp4* mutants

To examine how BMP4 acts in the patterning of ventral cell types, we analyzed a series of marker genes in *bmp4* mutant embryos. *dlx3* is expressed in the median fin fold of wildtype embryos at 24 hpf (Akimenko et al., 1994). A gap is observed in the ventral *dlx3* expression of stronger *bmp4^{st72}* mutant embryos, reflecting the loss of ventral tail fin in these mutants (Fig 2A–B). Some mutants additionally exhibit a loss of the dark staining at the caudal end of the yolk tube that apparently marks the cloaca. Despite a reduction in tail fin tissue, weakly affected mutant embryos exhibit uninterrupted *dlx3* expression. The most strongly affected *bmp4^{st72}* mutants also have a reduction in the extent of the expression of the endothelial marker *flk* (Thompson et al., 1998) in caudal regions of the tail (Fig 2C–D). To look for defects in tail somite formation we examined *myoD* expression (Weinberg et al., 1996). In mutants that display weak C1 dorsalization, somite formation is unaffected. However, in the strongest phenotypes, the caudal somites are ventrally fused across the midline (Fig 2E–F). The expression of markers of early dorsal and ventral fates, including *chordin*, *gooseoid*, *vox* and *vent*, are unaffected in *bmp4^{st72}* mutants at early stages (data not shown).

BMP signaling has recently been shown to be required for proper cloaca formation, although the endogenous BMP signal is unknown (Pyati et al., 2006). We thus examined markers for the pronephros (*pax2a*, (Krauss et al., 1991), which exits at the cloaca, and the cloaca itself (*prdm1*, (Wilm and Solnica-Krezel, 2005) *evx1*, (Thaeron et al., 2000) in *bmp4* mutants at 24hpf. As with the tail, there is variability in the phenotype of *bmp4^{st72}* and *bmp4^{st37}* homozygotes. In weaker mutants the expression of these genes is unaffected. However, *pax2a*, *evx1*, and *prdm1* expression are altered in more strongly dorsalized embryos. In these mutant embryos, the expression of *pax2a* in the pronephric terminus is altered. In wild-type embryos, *pax2a* is expressed in the pronephric terminus at the junction of the yolk sac and the tail fin (Fig 2G). In *bmp4* mutants, the pronephric terminus does not appear to exit the embryo (Fig 2H). Expression of the cloacal marker *evx1* is reduced and/or altered in pattern (Fig 2J) in more severe *bmp4^{st72}* mutants as compared to wildtype (Fig 2I). In addition, *prdm1* expression is reduced in the region of the cloaca and in the extension below the yolk tube (Fig 2K–L). It appears that in more severe *bmp4^{st72}* mutants, the cloaca does not form properly and the pronephric duct terminus fails to reach the exterior.

Pyati and colleagues presented evidence suggesting that the cloaca arises from the mesoderm posterior to the tailbud and demonstrated expansion of vascular and endothelial markers into that region at the 10-somite stage in embryos in which late BMP signaling was compromised (Pyati et al., 2006). We have examined the expression of the pronephric marker *pax2a* and the

erythroid precursor cell marker *gata1* at the 10-somite stage in *bmp4^{st72}* mutants. The expression of the pronephric marker *pax2a*, which is normally expressed in the mesoderm posterior to the tailbud, is only slightly if at all affected in *bmp4^{st72}* mutants (Fig 3A,B). In contrast, the expression of *gata1* is strikingly different in *bmp4^{st72}* mutants, which exhibit an apparent posterior expansion of blood precursors as compared to wild-type siblings (Fig 3C,D). Loss of BMP4 appears to cause a change in the fate of mesoderm posterior to the tailbud similar to that observed in embryos in which all BMP signaling was blocked during post-gastrula stages (Pyati et al., 2006).

bmp4 is the earliest gene known to be expressed in an asymmetrical manner in the heart field and has been suggested to be responsible for the left-right patterning of the heart (Chen et al., 1997; Schilling et al., 1999). Recently, injection of a *bmp4* splicing morpholino was shown to disrupt heart jogging in zebrafish (Chocron et al., 2007). In contrast, we find that *bmp4* is not required for early events in left-right patterning of the heart. At 24 hpf, examination of *bmp4* expression and morphological inspection demonstrated that the heart jogs to the left in both wild-type and *bmp4^{st72}* mutants (data not shown).

***bmp4*, *swr/bmp2b*, and *snh/bmp7* genetically interact**

To determine how the *bmp4*, *bmp2b*, and *bmp7* genes interact, we analyzed the phenotypes of embryos with various combinations of our null allele of *bmp4* (*bmp4^{st72}*), a null allele in *bmp2b* (*swr^{ta72}*) and a strong hypomorphic allele of *bmp7* (*snh^{ty68a}*). Although *bmp* signals are essential for tail development and *bmp2b* and *bmp7* mutants lack tails, some allelic combinations surprisingly resulted in embryo with ectopic tails (e.g. *swr^{ta72}/+*, *bmp4^{st72}/bmp4^{st72}*, Table 3). Similar ectopic or bifurcated tails were seen by Pyati et al. (Pyati et al., 2005) in a small fraction of embryos following loss of BMP signaling at midgastrula and postgastrula stages and by Connors and colleagues in some *mfn/tld* homozygotes (Connors et al., 1999). Interestingly, these bifurcated tails appear to develop only mesodermal and fin tissues (Pyati et al., 2005). Genotyping of embryos from a cross between a *swr^{ta72}*, *snh^{ty68a}*, *bmp4^{st72}* triple heterozygote and a *bmp4^{st72}* heterozygote suggested that this bifurcated tail phenotype is a dorsalized phenotype of intermediate strength, stronger than C1 but weaker than C2 (Table 3, Fig 4). Embryos with the strongest loss of BMP (*swr^{ta72}/+*, *bmp4^{st72}/bmp4^{st72}*, *snh^{ty68a}/+*) all displayed a C2 phenotype (Fig 4A). Embryos with slightly more BMP activity (*swr^{ta72}/+*, *bmp4^{st72}/+*, *snh^{ty68a}/+*, or *swr^{ta72}/+*, *bmp4^{st72}/bmp4^{st72}*) display C2 phenotypes, bifurcated tail phenotypes with cloacal defects (C1b, Fig 4B), or C1 phenotypes with strongly reduced tail fin and cloacal defects (C1s, Fig 4C), while embryos with even more BMP activity (*swr^{ta72}/+*; *bmp4^{st72}/+*) displayed C1 dorsalized phenotypes with either strongly (C1s) or weakly (C1w, Fig 4D) reduced tail fin. Further increases in BMP activity led to correspondingly weaker phenotypes (Fig 4E). A similar trend was observed in crosses with the *bmp4^{st37}* allele (data not shown). As a possible explanation of our data and the paradoxical ectopic tail, we considered a gradient model similar to that proposed for BMP function in ectoderm (Nguyen et al., 1998) in which the various allelic combinations alter the slope of the *bmp* gradient to a greater or lesser extent (see Fig 7A–C). In this model, the highest levels of BMP activity induce cloaca and ventral tail fin, and slightly lower levels induce other ventral fates including tail mesoderm and blood. This model predicts that intermediate reductions of *bmp* alter the slope of the BMP activity gradient such that the “slightly lower” levels of activity are present over a larger territory, resulting, for example, in the observed expansion of tail mesoderm.

Although there is extensive evidence indicating that BMP signals are essential to induce blood, the gradient model predicts that a slight reduction in BMP activity might lead to the expansion of blood fate. To determine if this was the case, we examined the expression of the erythrocyte precursor marker *gata1* in embryos from the same cross as above. As predicted, upon small reductions in BMP, such as in *bmp4^{st72}* homozygotes and *bmp4^{st72}/bmp4^{st72}*; *snh^{ty68a}/+*

embryos, *gata1* expression appears expanded compared to the wildtype pattern, extending into the region ventral to the tailbud where *gata1* expression is never observed in wildtype (Fig 5A–C). Further decreases in BMP, such as in *bmp4^{st72}/bmp4^{st72}; snh^{ty68a/+}; swr^{ta72/+}* mutants, also result in *gata1* expression in the region ventral to the tailbud, but the overall size of the *gata1* expression domain is progressively smaller as BMP activity is reduced (Fig 5D,E). This change in pattern is consistent with the reduction and ventral shift of the domain of cells fated to become blood that is predicted by a gradient model at lower levels of BMP activity. Combined, our results provide support for a gradient model of BMP function in which blood and tail mesoderm fates are induced at slightly lower BMP levels than ventral fin and cloaca.

Interestingly, the above analyses also demonstrated that *bmp4^{st72}* and *bmp4^{st37}* have stronger genetic interactions with *swr^{ta72}* than with *snh^{ty68a}*. *bmp4* mutants that are also lacking one copy of *bmp2b* (*bmp4^{st72}/bmp4^{st72}; swr^{ta72/+}*) display C2, C1b, or C1s phenotypes whereas *bmp4* mutants with one *snh* allele (*bmp4^{st72}/bmp4^{st72}; snh^{ty68a/+}*) predominantly fall within the C1w phenotypic category (Table 3). Furthermore, *gata1* expression in *bmp4* mutants that lack one copy of *bmp7* is expanded (*bmp4^{st72}/bmp4^{st72}; snh^{ty68a/+}*), similar to the phenotype in *bmp4* single mutants, whereas the expression domain of *gata1* is reduced in *bmp4^{st72}/bmp4^{st72}; swr^{ta72/+}* embryos, as is typical of more severely dorsialized embryos.

To determine whether *bmp4* functions redundantly with *bmp2b* and *bmp7*, we generated *swr^{ta72}, bmp4^{st72}, snh^{ty68a}* triple mutants. The triple mutants do not appear to be more severely dorsialized than *swr^{ta72}* single mutants. We saw no difference in morphology at the 1-somite stage. Furthermore, expression of *chordin*, which is expanded in maternal-zygotic *smad5* mutants at 40% epiboly (Kramer et al., 2002) but normal in *swr^{ta72}* mutants, is normal in triple mutants of the same stage (data not shown). In addition, at 2–3 somites the expression of *msxB*, which marks dorsal neuroectodermal tissue and is sensitive to variations in BMP activity (Schmid et al., 2000), in triple mutants is indistinguishable from that in *swr^{ta72}* single mutants (data not shown).

BMP4 does not regulate the expression of itself or other BMPs

BMP4 can activate its own expression in *Xenopus* overexpression experiments (Jones et al., 1992), and in zebrafish, both BMP2b and BMP7 are required for the maintenance of *bmp2b*, *bmp7*, and *bmp4* expression in ventral regions of developing embryos (Kishimoto et al., 1997; Schmid et al., 2000). We thus examined the expression of *bmp2b*, *bmp7*, and *bmp4* in *bmp4^{st72}* mutants between shield stage and 24hpf to determine whether zebrafish BMP4 also participates in this feedback loop (Fig 6). *bmp4* expression is unaffected in *bmp4^{st72}* mutants (Fig 6B,F), indicating that *bmp4* is not required to maintain its own expression. Nonsense mediated decay does not occur, presumably because the premature stop codon is located in the terminal exon (Thermann et al., 1998). The aforementioned loss of *bmp4* expression in *bmp4^{st37}* mutants (Fig 1C–F) is thus likely due to reduced transcription of the *bmp4* gene and/or reduced stability of the transcribed RNA.

BMP4 function is also not required for the maintenance of *bmp2b* or *bmp7* expression, as *bmp2b* and *bmp7* expression levels appear unaffected in *bmp4^{st72}* mutants at every stage examined (Fig 6C,D,G,H and data not shown). At 24hpf, *bmp2b* expression in the ventral tail fin is absent, but this is more likely to be due to an absence of that particular cell fate than a direct effect on *bmp2b* expression levels.

DISCUSSION

In this study, we have explored the role of BMP4 in zebrafish. We describe two alleles of *bmp4*: *bmp4^{st37}*, which we isolated in a forward genetic screen for dominant enhancers of *vox* and *vent*, and *bmp4^{st72}*, which we identified in a reverse genetic screen.

The role of *bmp4* in dorsoventral patterning

In mouse, BMP4 is the primary BMP required for early patterning. BMP4 knockout mice die very early, have little or no mesoderm and display truncated posterior structures (Winnier et al., 1995). In zebrafish, however, BMP2b and BMP7 appear to have taken over that role (Hammerschmidt et al., 1996; Kishimoto et al., 1997; Nguyen et al., 1998; Schmid et al., 2000). Because the expression of zebrafish *bmp4* is delayed in comparison with the expression of *bmp2b* and *bmp7* (Nikaido et al., 1997) and because no mutants in *bmp4* were identified in any of the large-scale morphological screens, the role of *bmp4* in zebrafish has been unclear. Our results demonstrate that zebrafish *bmp4* is required for proper ventroposterior fate specification. Although the phenotype is variable, *bmp4^{st72}* mutants display a loss of ventral tail fin, a reduction in endothelial precursor cells, ventral fusion of somites across the midline, and a failure of cloaca formation. However, at early stages, the expression of markers of dorsal and ventral fates, such as *chordin*, *goosecoid*, *vox*, *vent*, *bmp2b*, *bmp7*, and *bmp4* itself, are unaffected in *bmp4^{st72}* mutants. Thus, unlike *bmp2b* and *bmp7*, *bmp4* is not required for global dorsoventral patterning in zebrafish.

These results demonstrate that the early and late functions of BMP signaling in zebrafish (Pyati et al., 2005) involve different genes. We propose a model in which BMP2b and BMP7 are required for early patterning events and BMP2b and BMP4 are the essential regulators of late patterning (Fig 7D). Previous studies have shown that BMP2b and BMP7, probably functioning as heterodimers, specify ventral fates and allocate precursors to a tail domain. Complete loss of either BMP2b or BMP7 results in equivalent severely dorsalized phenotypes lacking ventral structures, and the two display cell-autonomous synergism in overexpression assays (Schmid et al., 2000). The putative BMP2b/BMP7 heterodimers likely act through Alk8 and Smad5, as maternal-zygotic *laf* and *sbm* mutants are severely dorsalized (Kramer et al., 2002; Mintzer et al., 2001). During this early phase, BMP2b and BMP7 activate their own expression as well as that of *smad1* and *bmp4* (Dick et al., 2000; Dick et al., 1999; Kishimoto et al., 1997; Nguyen et al., 1998; Schmid et al., 2000).

In the late gastrula and post-gastrula, we suggest that BMP2b and BMP4, acting additively and signaling through Smad1 and Smad5, specify ventroposterior fates, including the cloaca. The development of the tail fin is sensitive to *bmp2b* and *bmp4* dosages but not to *bmp7* dosage (Mullins et al., 1996 and this paper), and *bmp2b* and *bmp4* display a stronger genetic interaction than do *bmp4* and *bmp7* or *bmp2b* and *bmp7* (see Table 3). In addition, BMP2b and BMP4 belong to the same subfamily of BMPs and, unlike BMP2b and BMP7 or BMP4 and BMP7, do not exhibit synergism in overexpression assays (Schmid et al., 2000). These results are all consistent with a model in which *bmp2b* and *bmp4* have an additive, dosage dependent effect on patterning in the tail while *bmp7* interacts with *bmp4* only through the early effect of BMP7 on *bmp2b* and *bmp4* expression levels. An additive relationship between *bmp2b* and *bmp4* could also explain the variability in the *bmp4* mutant phenotype as well as in the heterozygous phenotype of *swr^{ta72}* if the relative contributions of *bmp2b* and *bmp4* to the total late BMP level vary between strains. In this later phase of BMP signaling, BMP activity is probably regulated by interactions between Chordin, Tolloid, and Sizzled. Both *chordin* and *tolloid* have been shown to be required after gastrulation in experiments with heat shock inducible *tolloid* (Connors et al., 2006), while the *sizzled* expression pattern, its mutant phenotype, and its function as a Tolloid antagonist suggest that Sizzled functions in the later phase as well (Martyn and Schulte-Merker, 2003; Muraoka et al., 2006; Yabe et al., 2003).

BMPs function as morphogens in mesendodermal tail patterning

Alterations in neural crest fate in embryos with differences in BMP activity have provided genetic evidence that BMPs act as morphogens in the ectoderm (Nguyen et al., 1998). Although it has been postulated that BMPs act as morphogens in the mesendoderm during tail

development (Connors et al., 2006; Kramer et al., 2002; Pyati et al., 2006), the evidence for this has not been as strong as for earlier stages. Our results provide evidence in support of a model in which BMPs act as morphogens in the mesendoderm, with cloaca and tail fin requiring the absolute highest levels of BMP signaling, while blood and tail mesoderm require slightly lower, but still high, levels of BMP (Fig 7A). This model for late BMP function eliminates the need to invoke a new function for BMPs in inhibiting secondary tails at the end of gastrulation (Pyati et al., 2006; Pyati et al., 2005), which is in striking contrast to the requirement for BMP function in tail specification a few hours earlier.

We have carefully examined the phenotypes of embryos in which BMP levels have been genetically altered. Our data demonstrate that the bifurcated tail phenotype first noted by Connors and colleagues in *mfn/tld* homozygotes (Connors et al., 1999) and further defined by Pyati and colleagues (Pyati et al., 2005) lies within the continuum of dorsalized phenotypes, stronger than the C1 but weaker than the C2 dorsalized phenotype (Table 3; Fig 4). Thus, upon progressive loss of BMP, expansion of tail mesoderm precedes the reduction of tail mesoderm seen in C2 dorsalized embryos. We also provide evidence that blood fate is first expanded and then reduced as BMP function is progressively lost (Fig 5). Furthermore, the tail fin and cloaca appear to be the most sensitive to alterations in BMP signaling, as those fates are the first to be lost when BMP signaling is genetically reduced (Table 3, Fig 4 and data not shown). All of our results are explained by graded action of BMPs in mesoderm patterning and the postulate that different allelic combinations alter the slope of the BMP gradient, with intermediate reductions in BMP causing a larger region of the dorsoventral axis to fall within the upper and lower thresholds for tail mesoderm and blood fates (Fig 7A–C). Other factors, such as Nodals, Wnts and Fgfs, also contribute to the patterning of the tail, perhaps by differentiating between tail mesoderm and blood fates.

Dominant enhancer screen and genetic background differences

In our screen for dominant enhancers of *vox* and *vent*, we identified at least three, and probably four, new alleles of *sbn/smud5* (*st30*, *st31*, *st32*, *st33*). Zygotic BMP signals are required for the maintenance of *vox* and *vent* expression in the midgastrula (Kawahara et al., 2000a; Kawahara et al., 2000b; Melby et al., 2000), while *vox* and *vent* repress *chd* expression, thereby indirectly activating *bmp* expression (Imai et al., 2001). Thus, the isolation of alleles of *sbn/smud5*, which is a component of the *bmp* signaling pathway, demonstrates the efficacy of dominant enhancer screens for identifying interacting genes. The identification of our insertional allele of *bmp4* (*st37*) reflects the utility of the dominant enhancer screen, as it might have been missed in classical forward genetic screens given that the phenotype of *bmp4^{st37}* in a wild-type *vox* background is variable in penetrance and expressivity, with some stocks failing to exhibit any observable morphological phenotype in *bmp^{st37}* mutants.

The dependence of phenotype on genetic background is not unprecedented. We performed our screen in a TL background because the penetrance and expressivity of *Df^{st7}* mutants as well as *vox* and *vent* morphants are significantly more severe in the TL strain as compared to the AB and WIK strains (Imai et al., 2001). In addition, the *swr^{ta72}* (*bmp2b*) mutation displays a dominant zygotic C1 dorsalized phenotype in some, but not all, backgrounds, and the phenotypic strength of *snh^{ty68a}* (*bmp7*) homozygotes varies between fish (Mullins et al., 1996). In the course of our mapping experiments, we localized modifiers of dorsoventral patterning phenotypes to LG10, near the *vox* and *vent* homolog *ved*, and LG11, near *bmp7* (H.L.S. and W.S.T, unpublished data). Neither modifier displays a recessive phenotype in otherwise wild-type embryos, but we see enhancement of the dorsalization caused by other mutations, including *Df^{st7}* (LG10) and *swr^{ta72}*, *snh^{ty68a}*, *sbn^{st31}*, *sbn^{st32}*, and *bmp4^{st37}* (LG11), in the presence of these enhancers. We have not identified the specific genes that are changed

in different backgrounds, but sequence variations resulting in slight alterations in *ved* and *bmp7* mRNA level or protein activity are possibilities.

Finally, an interesting possibility is that *bmp4^{st37}* may be a background modifier itself. Premeiotic ENU mutagenesis typically causes point mutations in zebrafish (Wienholds et al., 2002), so it is unexpected that we obtained an insertion allele in a premeiotic ENU mutagenesis screen. Furthermore, the insertion appears to have originated from LG8, indicating chromosomal rearrangement. Thus, *bmp4^{st37}* may be a spontaneous mutation rather than one induced by our ENU mutagenesis. A second possibility is that the *bmp4^{st37}* mutation derived from the tester *Df^{st7}* male rather than the ENU-mutagenized parent. The *Df^{st7}* allele was produced via postmeiotic ENU mutagenesis, which does cause frequent chromosomal rearrangements (Imai et al., 2000).

Conclusions

Our results demonstrate that zebrafish *bmp4* is essential for proper ventroposterior patterning of the zebrafish embryo. We present a model for *bmp4* function in which *bmp4* cooperates with *bmp2b* to pattern ventroposterior fates including ventral tail fin, cloaca, blood, and tail mesoderm. We also offer evidence that BMPs function as morphogens to pattern the mesoderm in the late phase of BMP signaling, with the highest levels of BMP signaling required for ventral tail fin and cloaca development, and slightly lower levels for blood and tail mesoderm. Finally, the *bmp4* alleles we have identified are viable in some genetic backgrounds and as such can be used to investigate other, later processes in which *bmp4* is believed to play a role.

Supplementary Material

Refer to Web version on PubMed Central for supplementary material.

Acknowledgements

We thank David Kimelman and Mary Mullins for generously providing in situ hybridization probes; Alex Schier, Ian Woods, and members of our groups for comments on the manuscript; Naomi Arana for technical help with the reverse genetic screen; Naomi Arana, Isaac Middendorf, Tuky Reyes, Claudia Dominguez, Ali Brincat, and Chenelle Hill for excellent fish care. This work was supported by NIH grants HG002995 (C.B.M.) and HG002568 (W.S.T.). H.L.S was funded by a predoctoral fellowship grant from Howard Hughes Medical Institute.

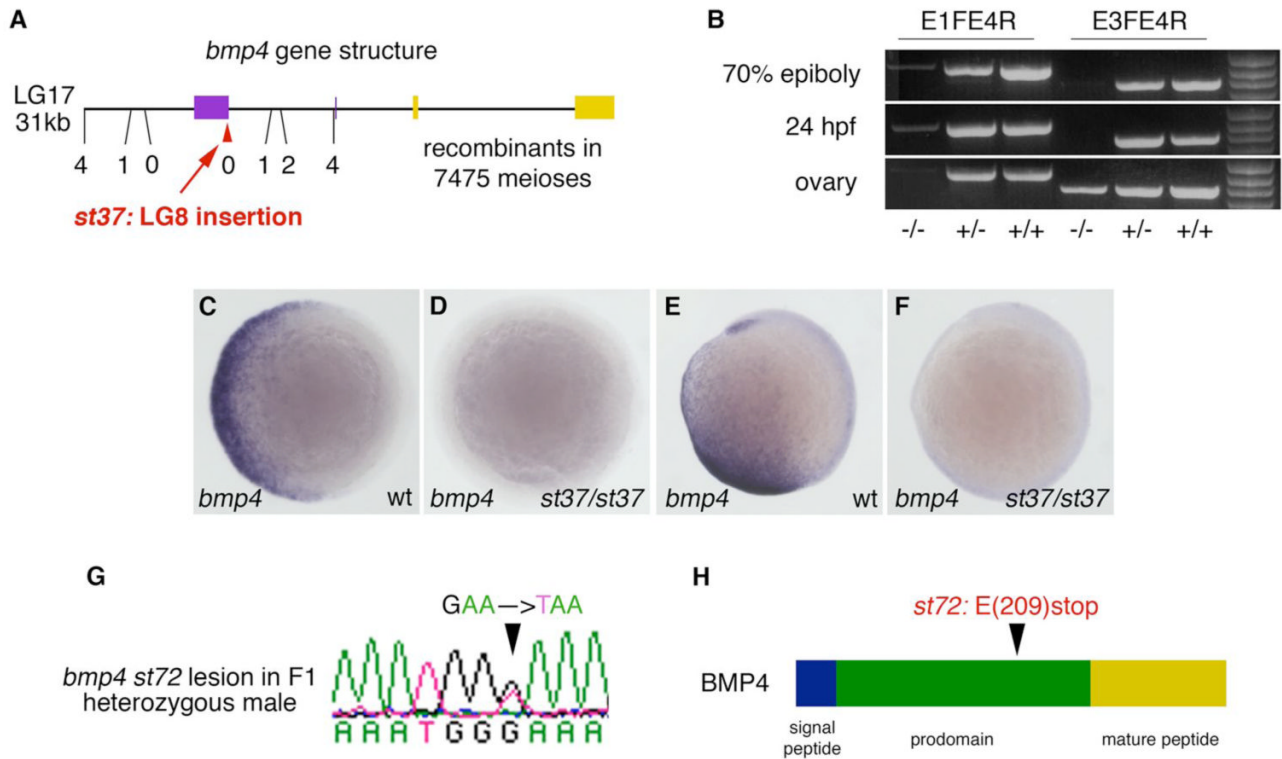
References

- Akimenko MA, Ekker M, Wegner J, Lin W, Westerfield M. Combinatorial expression of three zebrafish genes related to distal-less: part of a homeobox gene code for the head. *J Neurosci* 1994;14:3475–86. [PubMed: 7911517]
- Chen JN, van Eeden FJ, Warren KS, Chin A, Nusslein-Volhard C, Haffter P, Fishman MC. Left-right pattern of cardiac BMP4 may drive asymmetry of the heart in zebrafish. *Development* 1997;124:4373–82. [PubMed: 9334285]
- Chen KS, Gould MN. Development of a universal gap repair vector for yeast-based screening of knockout rodents. *Biotechniques* 2004;37:383–8. [PubMed: 15470892]
- Chocron S, Verhoeven MC, Rentzsch F, Hammerschmidt C, Bakkens J. Zebrafish Bmp4 regulates left-right asymmetry at two distinct developmental time points. *Dev Biol* 2007;305:577–588. [PubMed: 17395172]
- Connors SA, Trout J, Ekker M, Mullins MC. The role of tolloid/mini fin in dorsoventral pattern formation of the zebrafish embryo. *Development* 1999;126:3119–30. [PubMed: 10375503]
- Connors SA, Tucker JA, Mullins MC. Temporal and spatial action of tolloid (mini fin) and chordin to pattern tail tissues. *Dev Biol* 2006;293:191–202. [PubMed: 16530746]
- Dale L, Howes G, Price BM, Smith JC. Bone morphogenetic protein 4: a ventralizing factor in early *Xenopus* development. *Development* 1992;115:573–85. [PubMed: 1425340]

- Dick A, Hild M, Bauer H, Imai Y, Maifeld H, Schier AF, Talbot WS, Bouwmeester T, Hammerschmidt M. Essential role of Bmp7 (snailhouse) and its prodomain in dorsoventral patterning of the zebrafish embryo. *Development* 2000;127:343–54. [PubMed: 10603351]
- Dick A, Meier A, Hammerschmidt M. Smad1 and Smad5 have distinct roles during dorsoventral patterning of the zebrafish embryo. *Dev Dyn* 1999;216:285–98. [PubMed: 10590480]
- Fainsod A, Steinbeisser H, De Robertis EM. On the function of BMP-4 in patterning the marginal zone of the *Xenopus* embryo. *Embo J* 1994;13:5015–25. [PubMed: 7957067]
- Fekany K, Yamanaka Y, Leung T, Sirotkin HI, Topczewski J, Gates MA, Hibi M, Renucci A, Stemple D, Radbill A, Schier AF, Driever W, Hirano T, Talbot WS, Solnica-Krezel L. The zebrafish bozozok locus encodes Dharma, a homeodomain protein essential for induction of gastrula organizer and dorsoanterior embryonic structures. *Development* 1999;126:1427–38. [PubMed: 10068636]
- Geisler R, Rauch GJ, Baier H, van Bebber F, Bross L, Dekens MP, Finger K, Fricke C, Gates MA, Geiger H, Geiger-Rudolph S, Gilmour D, Glaser S, Gnugge L, Habeck H, Hingst K, Holley S, Keenan J, Kirm A, Knaut H, Lashkari D, Maderspacher F, Martyn U, Neuhauss S, Neumann C, Nicolson T, Pelegri F, Ray R, Rick JM, Roehl H, Roeser T, Schauerte HE, Schier AF, Schonberger U, Schonhaler HB, Schulte-Merker S, Seydler C, Talbot WS, Weiler C, Nusslein-Volhard C, Haffter P. A radiation hybrid map of the zebrafish genome. *Nat Genet* 1999;23:86–9. [PubMed: 10471505]
- Graff JM, Thies RS, Song JJ, Celeste AJ, Melton DA. Studies with a *Xenopus* BMP receptor suggest that ventral mesoderm-inducing signals override dorsal signals in vivo. *Cell* 1994;79:169–79. [PubMed: 7522972]
- Hammerschmidt M, Serbedzija GN, McMahon AP. Genetic analysis of dorsoventral pattern formation in the zebrafish: requirement of a BMP-like ventralizing activity and its dorsal repressor. *Genes Dev* 1996;10:2452–61. [PubMed: 8843197]
- Hibi M, Hirano T, Dawid IB. Organizer formation and function. *Results Probl Cell Differ* 2002;40:48–71. [PubMed: 12353486]
- Hukriede N, Fisher D, Epstein J, Joly L, Tellis P, Zhou Y, Barbazuk B, Cox K, Fenton-Noriega L, Hersey C, Miles J, Sheng X, Song A, Waterman R, Johnson SL, Dawid IB, Chevrette M, Zon LI, McPherson J, Ekker M. The LN54 radiation hybrid map of zebrafish expressed sequences. *Genome Res* 2001;11:2127–32. [PubMed: 11731504]
- Imai Y, Feldman B, Schier AF, Talbot WS. Analysis of chromosomal rearrangements induced by postmeiotic mutagenesis with ethylnitrosourea in zebrafish. *Genetics* 2000;155:261–72. [PubMed: 10790400]
- Imai Y, Gates MA, Melby AE, Kimelman D, Schier AF, Talbot WS. The homeobox genes *vox* and *vent* are redundant repressors of dorsal fates in zebrafish. *Development* 2001;128:2407–20. [PubMed: 11493559]
- Jasuja R, Voss N, Ge G, Hoffman GG, Lyman-Gingerich J, Pelegri F, Greenspan DS. *bmp1* and *mini fin* are functionally redundant in regulating formation of the zebrafish dorsoventral axis. *Mech Dev* 2006;123:548–58. [PubMed: 16824737]
- Jones CM, Lyons KM, Lapan PM, Wright CV, Hogan BL. DVR-4 (bone morphogenetic protein-4) as a posterior-ventralizing factor in *Xenopus* mesoderm induction. *Development* 1992;115:639–47. [PubMed: 1425343]
- Kawahara A, Wilm T, Solnica-Krezel L, Dawid IB. Antagonistic role of *vega1* and *bozozok/dharma* homeobox genes in organizer formation. *Proc Natl Acad Sci U S A* 2000a;97:12121–6. [PubMed: 11050240]
- Kawahara A, Wilm T, Solnica-Krezel L, Dawid IB. Functional interaction of *vega2* and *gooseoid* homeobox genes in zebrafish. *Genesis* 2000b;28:58–67. [PubMed: 11064422]
- Kishimoto Y, Lee KH, Zon L, Hammerschmidt M, Schulte-Merker S. The molecular nature of zebrafish swirl: BMP2 function is essential during early dorsoventral patterning. *Development* 1997;124:4457–66. [PubMed: 9409664]
- Koos DS, Ho RK. The *nieuwkoid/dharma* homeobox gene is essential for *bmp2b* repression in the zebrafish pregastrula. *Dev Biol* 1999;215:190–207. [PubMed: 10545230]
- Kramer C, Mayr T, Nowak M, Schumacher J, Runke G, Bauer H, Wagner DS, Schmid B, Imai Y, Talbot WS, Mullins MC, Hammerschmidt M. Maternally supplied Smad5 is required for ventral

- specification in zebrafish embryos prior to zygotic Bmp signaling. *Dev Biol* 2002;250:263–79. [PubMed: 12376102]
- Krauss S, Johansen T, Korzh V, Fjose A. Expression pattern of zebrafish pax genes suggests a role in early brain regionalization. *Nature* 1991;353:267–70. [PubMed: 1680220]
- Little SC, Mullins MC. Twisted gastrulation promotes BMP signaling in zebrafish dorsal-ventral axial patterning. *Development* 2004;131:5825–35. [PubMed: 15525664]
- Martyn U, Schulte-Merker S. The ventralized ogon mutant phenotype is caused by a mutation in the zebrafish homologue of Sizzled, a secreted Frizzled-related protein. *Dev Biol* 2003;260:58–67. [PubMed: 12885555]
- Melby AE, Beach C, Mullins M, Kimelman D. Patterning the early zebrafish by the opposing actions of bozozok and vox/vent. *Dev Biol* 2000;224:275–85. [PubMed: 10926766]
- Mintzer KA, Lee MA, Runke G, Trout J, Whitman M, Mullins MC. Lost-a-fin encodes a type I BMP receptor, Alk8, acting maternally and zygotically in dorsoventral pattern formation. *Development* 2001;128:859–69. [PubMed: 11222141]
- Mullins MC, Hammerschmidt M, Kane DA, Odenthal J, Brand M, van Eeden FJ, Furutani-Seiki M, Granato M, Haffter P, Heisenberg CP, Jiang YJ, Kelsh RN, Nusslein-Volhard C. Genes establishing dorsoventral pattern formation in the zebrafish embryo: the ventral specifying genes. *Development* 1996;123:81–93. [PubMed: 9007231]
- Muraoka O, Shimizu T, Yabe T, Nojima H, Bae YK, Hashimoto H, Hibi M. Sizzled controls dorsoventral polarity by repressing cleavage of the Chordin protein. *Nat Cell Biol* 2006;8:329–38. [PubMed: 16518392]
- Neave B, Holder N, Patient R. A graded response to BMP-4 spatially coordinates patterning of the mesoderm and ectoderm in the zebrafish. *Mech Dev* 1997;62:183–95. [PubMed: 9152010]
- Nguyen VH, Schmid B, Trout J, Connors SA, Ekker M, Mullins MC. Ventral and lateral regions of the zebrafish gastrula, including the neural crest progenitors, are established by a bmp2b/swirl pathway of genes. *Dev Biol* 1998;199:93–110. [PubMed: 9676195]
- Nikaido M, Tada M, Saji T, Ueno N. Conservation of BMP signaling in zebrafish mesoderm patterning. *Mech Dev* 1997;61:75–88. [PubMed: 9076679]
- Postlethwait JH, Talbot WS. Zebrafish genomics: from mutants to genes. *Trends Genet* 1997;13:183–90. [PubMed: 9154001]
- Piyati UJ, Cooper MS, Davidson AJ, Nechiporuk A, Kimelman D. Sustained Bmp signaling is essential for cloaca development in zebrafish. *Development* 2006;133:2275–84. [PubMed: 16672335]
- Piyati UJ, Webb AE, Kimelman D. Transgenic zebrafish reveal stage-specific roles for Bmp signaling in ventral and posterior mesoderm development. *Development* 2005;132:2333–43. [PubMed: 15829520]
- Reim G, Brand M. Maternal control of vertebrate dorsoventral axis formation and epiboly by the POU domain protein Spg/Pou2/Oct4. *Development* 2006;133:2757–70. [PubMed: 16775002]
- Ryu SL, Fujii R, Yamanaka Y, Shimizu T, Yabe T, Hirata T, Hibi M, Hirano T. Regulation of dharma/bozozok by the Wnt pathway. *Dev Biol* 2001;231:397–409. [PubMed: 11237468]
- Schilling TF, Concordet JP, Ingham PW. Regulation of left-right asymmetries in the zebrafish by Shh and BMP4. *Dev Biol* 1999;210:277–87. [PubMed: 10357891]
- Schmid B, Furthauer M, Connors SA, Trout J, Thisse B, Thisse C, Mullins MC. Equivalent genetic roles for bmp7/snailhouse and bmp2b/swirl in dorsoventral pattern formation. *Development* 2000;127:957–67. [PubMed: 10662635]
- Schmidt JE, Suzuki A, Ueno N, Kimelman D. Localized BMP-4 mediates dorsal/ventral patterning in the early *Xenopus* embryo. *Dev Biol* 1995;169:37–50. [PubMed: 7750652]
- Schulte-Merker S, Lee KJ, McMahon AP, Hammerschmidt M. The zebrafish organizer requires chordino. *Nature* 1997;387:862–3. [PubMed: 9202118]
- Shentu H, Wen HJ, Her GM, Huang CJ, Wu JL, Hwang SP. Proximal upstream region of zebrafish bone morphogenetic protein 4 promoter directs heart expression of green fluorescent protein. *Genesis* 2003;37:103–12. [PubMed: 14595833]
- Shimizu T, Yamanaka Y, Nojima H, Yabe T, Hibi M, Hirano T. A novel repressor-type homeobox gene, ved, is involved in dharma/bozozok-mediated dorsal organizer formation in zebrafish. *Mech Dev* 2002;118:125–38. [PubMed: 12351176]

- Shimoda N, Knapik EW, Ziniti J, Sim C, Yamada E, Kaplan S, Jackson D, de Sauvage F, Jacob H, Fishman MC. Zebrafish genetic map with 2000 microsatellite markers. *Genomics* 1999;58:219–32. [PubMed: 10373319]
- Sidi S, Goutel C, Peyrieras N, Rosa FM. Maternal induction of ventral fate by zebrafish radar. *Proc Natl Acad Sci U S A* 2003;100:3315–20. [PubMed: 12601179]
- Sirotkin HI, Dougan ST, Schier AF, Talbot WS. *bozozok* and *squint* act in parallel to specify dorsal mesoderm and anterior neuroectoderm in zebrafish. *Development* 2000;127:2583–92. [PubMed: 10821757]
- Suzuki A, Thies RS, Yamaji N, Song JJ, Wozney JM, Murakami K, Ueno N. A truncated bone morphogenetic protein receptor affects dorsal-ventral patterning in the early *Xenopus* embryo. *Proc Natl Acad Sci U S A* 1994;91:10255–9. [PubMed: 7937936]
- Talbot WS, Schier AF. Positional cloning of mutated zebrafish genes. *Methods Cell Biol* 1999;60:259–86. [PubMed: 9891342]
- Thaeron C, Avaron F, Casane D, Borday V, Thisse B, Thisse C, Boulekbache H, Laurenti P. Zebrafish *evx1* is dynamically expressed during embryogenesis in subsets of interneurons, posterior gut and urogenital system. *Mech Dev* 2000;99:167–72. [PubMed: 11091087]
- Thermann R, Neu-Yilik G, Deters A, Frede U, Wehr K, Hagemeyer C, Hentze MW, Kulozik AE. Binary specification of nonsense codons by splicing and cytoplasmic translation. *Embo J* 1998;17:3484–94. [PubMed: 9628884]
- Thompson MA, Ransom DG, Pratt SJ, MacLennan H, Kieran MW, Detrich HW 3rd, Vail B, Huber TL, Paw B, Brownlie AJ, Oates AC, Fritz A, Gates MA, Amores A, Bahary N, Talbot WS, Her H, Beier DR, Postlethwait JH, Zon LI. The *cloche* and *spadetail* genes differentially affect hematopoiesis and vasculogenesis. *Dev Biol* 1998;197:248–69. [PubMed: 9630750]
- van Eeden FJ, Granato M, Odenthal J, Haffter P. Developmental mutant screens in the zebrafish. *Methods Cell Biol* 1999;60:21–41. [PubMed: 9891329]
- Weinberg ES, Allende ML, Kelly CS, Abdelhamid A, Murakami T, Andermann P, Doerre OG, Grunwald DJ, Riggleman B. Developmental regulation of zebrafish *MyoD* in wild-type, no tail and *spadetail* embryos. *Development* 1996;122:271–80. [PubMed: 8565839]
- Wienholds E, Schulte-Merker S, Walderich B, Plasterk RH. Target-selected inactivation of the zebrafish *rag1* gene. *Science* 2002;297:99–102. [PubMed: 12098699]
- Wilm TP, Solnica-Krezel L. Essential roles of a zebrafish *prdm1/blimp1* homolog in embryo patterning and organogenesis. *Development* 2005;132:393–404. [PubMed: 15623803]
- Winnier G, Blessing M, Labosky PA, Hogan BL. Bone morphogenetic protein-4 is required for mesoderm formation and patterning in the mouse. *Genes Dev* 1995;9:2105–16. [PubMed: 7657163]
- Woods IG, Kelly PD, Chu F, Ngo-Hazelett P, Yan YL, Huang H, Postlethwait JH, Talbot WS. A comparative map of the zebrafish genome. *Genome Res* 2000;10:1903–14. [PubMed: 11116086]
- Yabe T, Shimizu T, Muraoka O, Bae YK, Hirata T, Nojima H, Kawakami A, Hirano T, Hibi M. *Ogon/Secreted Frizzled* functions as a negative feedback regulator of *Bmp* signaling. *Development* 2003;130:2705–16. [PubMed: 12736214]
- Zan Y, Haag JD, Chen KS, Shepel LA, Wigington D, Wang YR, Hu R, Lopez-Guajardo CC, Brose HL, Porter KI, Leonard RA, Hitt AA, Schommer SL, Elegbede AF, Gould MN. Production of knockout rats using ENU mutagenesis and a yeast-based screening assay. *Nat Biotechnol* 2003;21:645–51. [PubMed: 12754522]

**Figure 1.**

Two alleles of zebrafish *bmp4*. *st37* (A–F) is an insertion allele of *bmp4* isolated in a screen for dominant enhancers of *vox* and *vent*; *st72* (G,H) is a null allele identified in a reverse genetic screen with a yeast-based truncation assay. (A) Physical map of an approximately 31 kb region on LG17 that contains the four known exons of *bmp4*. Noncoding exons are purple, coding exons are yellow. The location and number of recombinants in 7475 meioses is shown for the SNP markers used in high resolution mapping of *st37*. The red arrowhead denotes the insertion site. (B) RT-PCR on total RNA from 70% epiboly embryos, 24hr embryos, and dissected ovaries with primers in exon 1 and exon 4 (3' of the insertion) and primers in exon 3 and exon 4 (coding region) of *bmp4*. *bmp4* mRNA is significantly reduced in *st37* homozygous mutants at both 70% epiboly and 24hpf as compared to wild-type and heterozygous embryos. The reduction of *bmp4* mRNA is less extreme in *st37* mutant ovaries when assayed with primers within the coding region of *bmp4*, suggesting the existence of *bmp4* isoforms with alternate 5' UTR in mutant ovaries. (C–F) *bmp4* expression in *bmp4^{st37}* homozygotes (D,F) and wild-type siblings (C,E). (C,D) Shield stage, animal pole view, dorsal to the right. (E,F) Bud stage, lateral view, dorsal to the right. (G) A sequencing trace from the *st72* F1 heterozygous male identifies a G to T mutation in the fourth exon of *bmp4* that changes Glu(209) to a stop. (H) Schematic representation of the BMP4 protein and the location of the *st72* lesion. The *bmp4^{st72}* lesion causes the BMP4 protein to truncate in the prodomain.

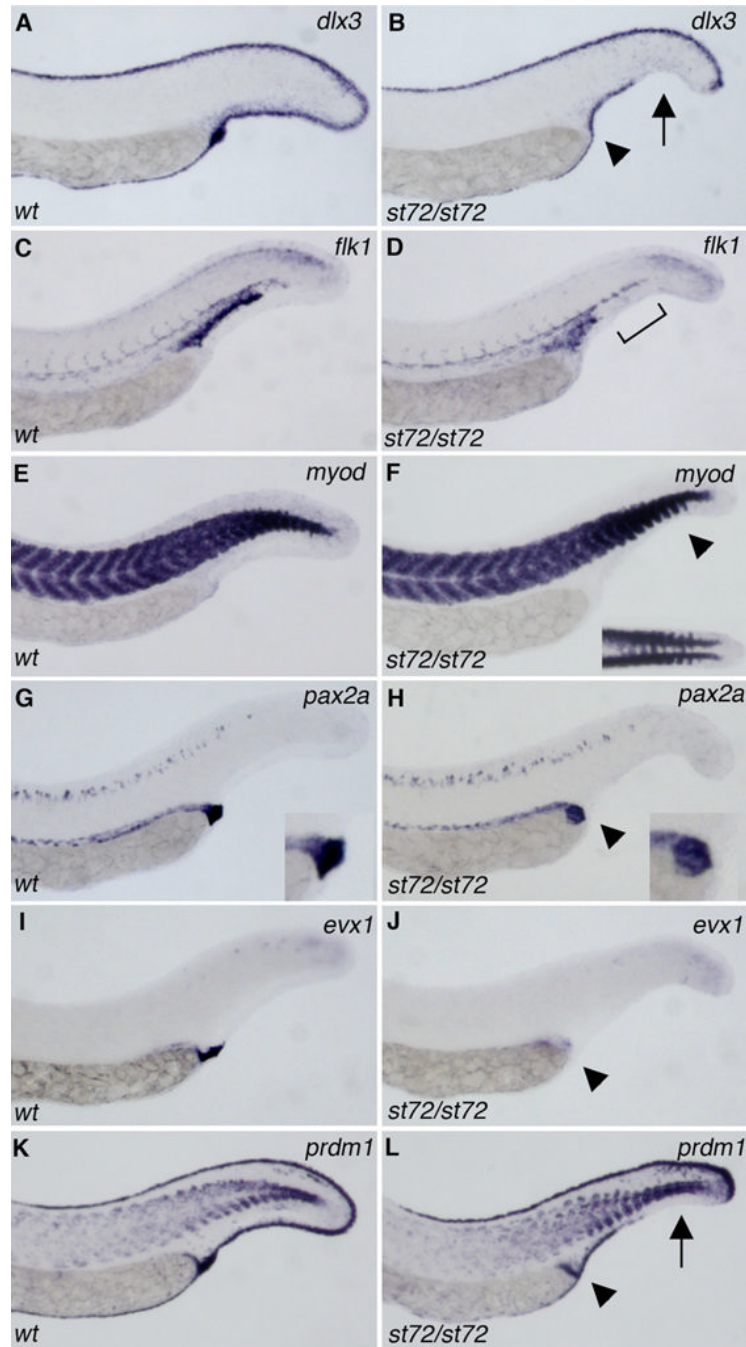


Figure 2.

Tail patterning is affected in *bmp4* mutants. *dlx3* (A,B), *flk1* (C,D) *myod* (E,F), *pax2a* (G,H), *evx1* (I,J) and *prdm1* (K,L) expression in 26 hpf wild-type (A, C, E, G, I, K) and *bmp4^{st72}* mutant (B, D, F, H, J, L) embryos. Gaps in *dlx3* and *prdm1* expression in the tail fin (arrow) and reduction of staining in the cloacal region (arrowhead) are apparent in *bmp4^{st72}* mutants (B, L). There is also a reduction in the extent of the *flk1* expression domain in the tail of *bmp4* mutants (D, bracket). Tail somites are fused across the ventral midline (F, arrowhead, inset) and the pronephric terminus is slightly altered in shape and location (H, arrowhead) in *bmp4^{st72}* mutants. Expression of *evx1* is reduced and more internal in *bmp4^{st72}* mutants (J)

than in wild-type embryos (I). All views are lateral with anterior to the left except the inset in F, which is a dorsal view.

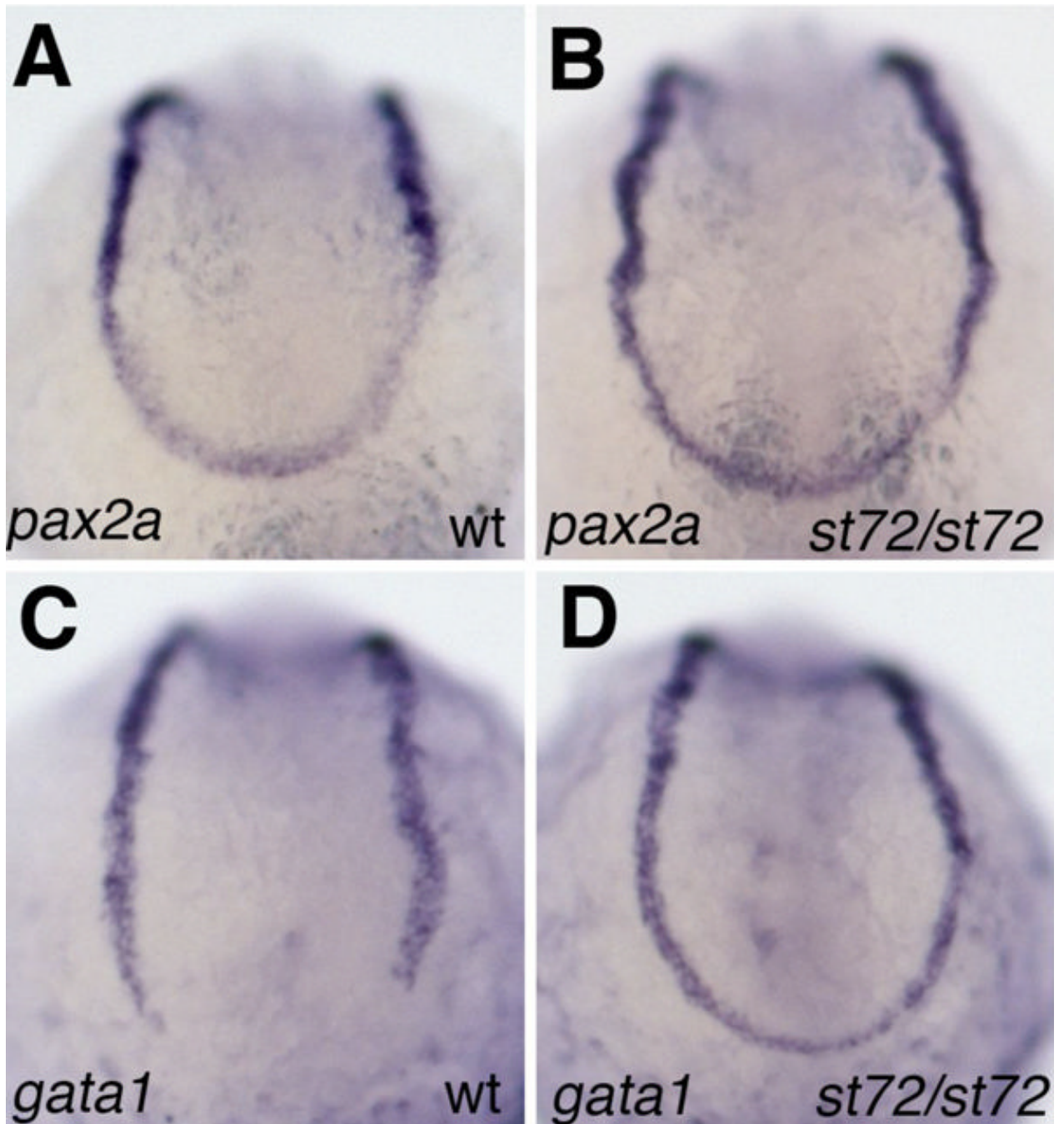


Figure 3.

Expansion of blood fates in *bmp4^{st72}* mutants. (A,B) Expression of *pax2a* in *bmp^{st72}* mutants (B) and wild-type siblings (A) at the 10-somite stage. The expression of *pax2a* appears slightly upregulated in the mesoderm below the tailbud. (C,D) *gata1* expression in *bmp^{st72}* mutants (D) and wild-type siblings (C) at the 10-somite stage. In *bmp^{st72}* mutants, but not in their wild-type siblings, *gata1* expression extends all the way around the tailbud.

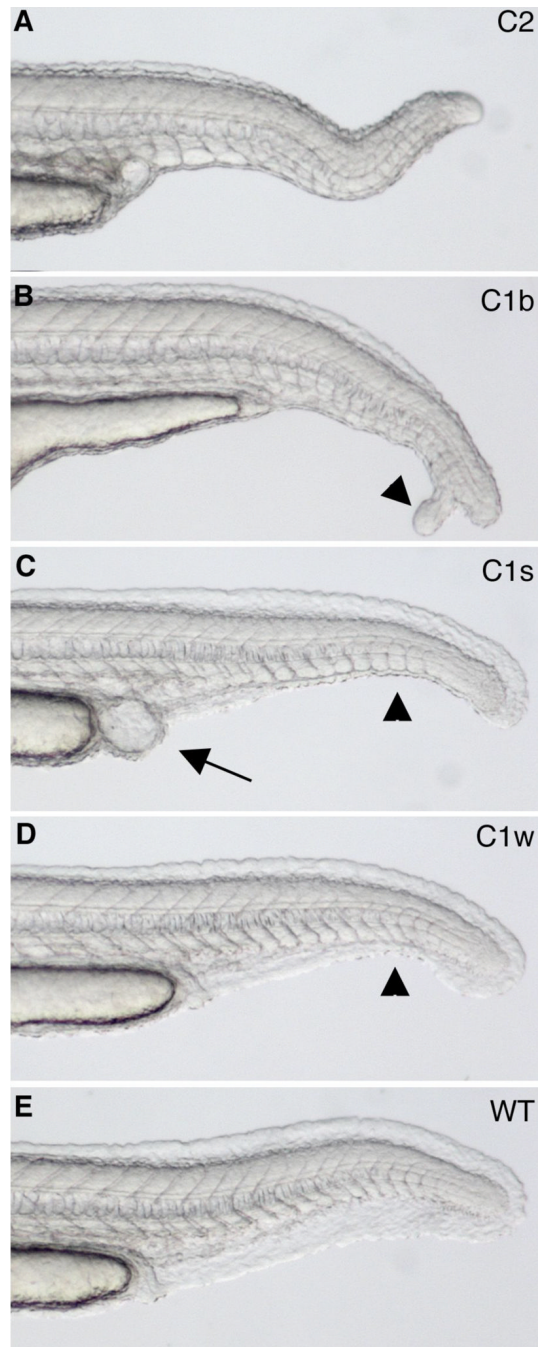


Figure 4. Morphology of the tail of live 28 hpf embryos from crosses with *swr^{ta72}*, *snh^{ty68a}* and *bmp4^{st72}* or *bmp4^{st37}*. (A) C2 phenotype. (B) C1b phenotype with a bifurcated tail (arrowhead). (C) Strong C1 (C1s) phenotype in which more than half of the tail fin is lost (arrowhead). Cloacal defects are also apparent (arrow). (D) Weak C1 (C1w) phenotype displaying a slight reduction in ventral tail fin (arrowhead). (E) Wild-type phenotype. Anterior is to the left.

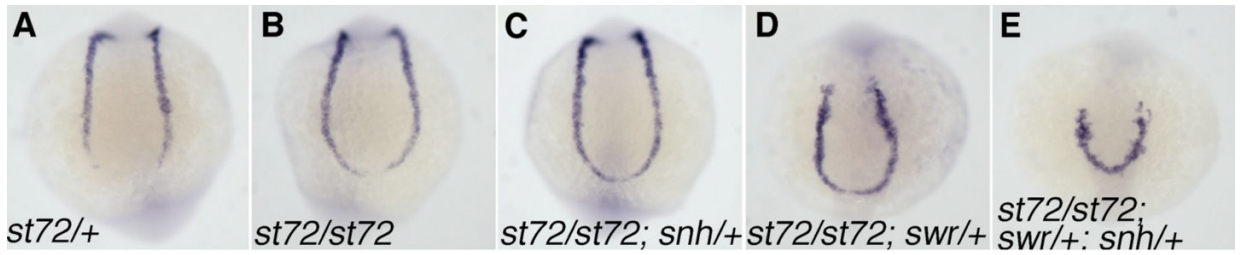


Figure 5.

Blood fate is first expanded and then reduced upon progressive loss of BMP activity. *gata1* expression at 10 somites in embryos from a cross between a triple *bmp* heterozygote and a *bmp4^{st72}* heterozygote. (A) Wild-type phenotype exhibited by a *bmp4^{st72}* heterozygote. Expansion of the *gata1* expression domain ventral to the tailbud is evident in a *bmp4^{st72}* homozygote (B) and a *bmp4^{st72}/bmp4^{st72}; snh^{ty68a/+}* embryo (C). Reduction of the *gata1* expression domain is observed upon further reduction of BMP, as in these *bmp4^{st72}/bmp4^{st72}; swr^{ta72/+}* (D) and *bmp4^{st72}/bmp4^{st72}; snh^{ty68a/+}; swr^{ta72/+}* (E) embryos, although ectopic *gata1* expression ventral to the tailbud is still apparent.

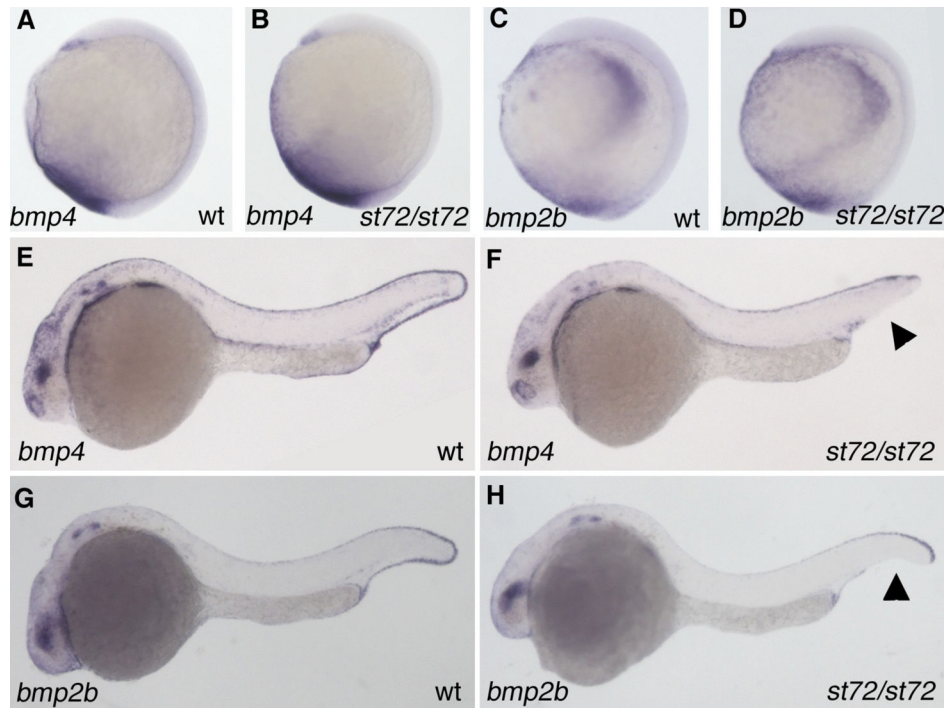
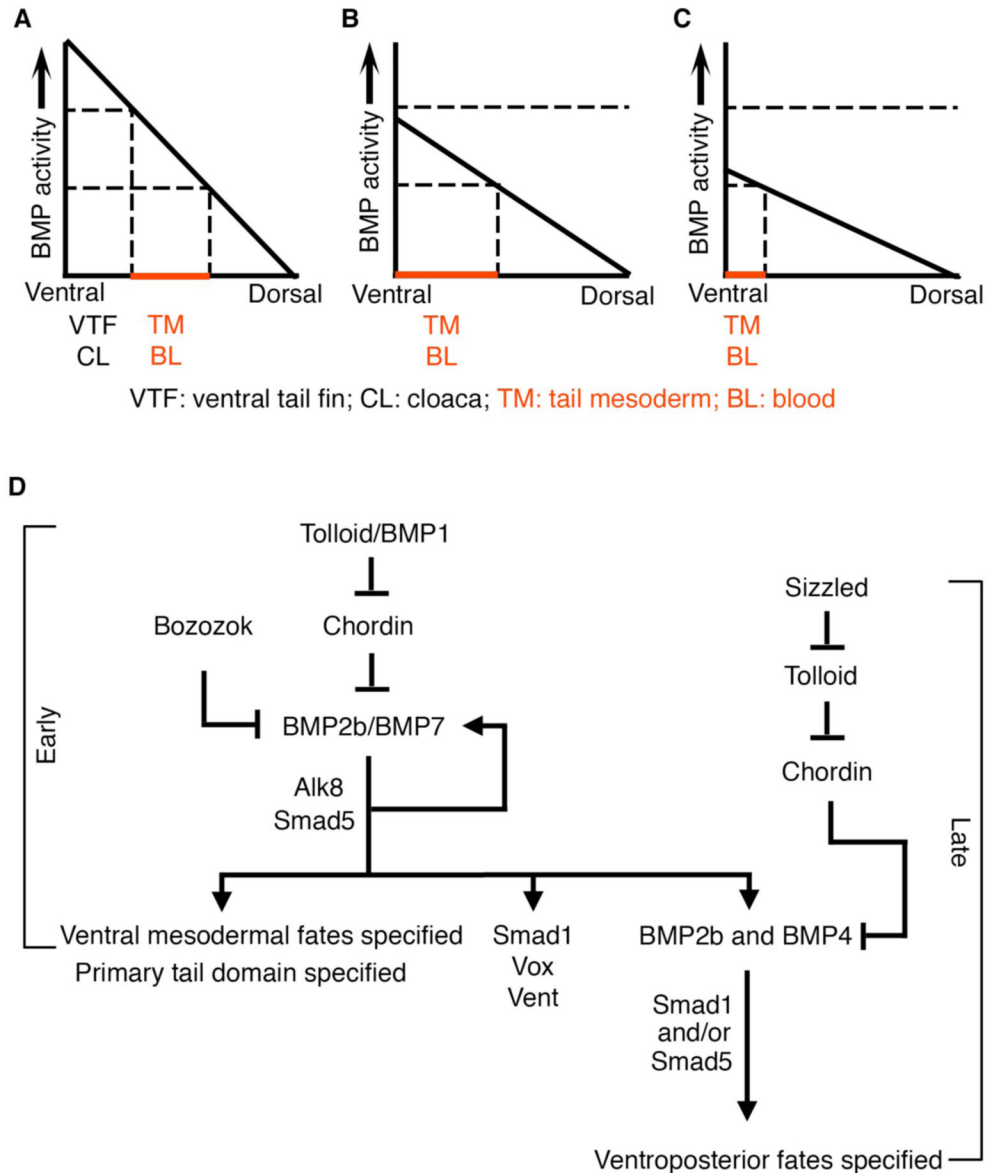


Figure 6.

bmp expression is unaffected in *bmp4* mutants. *bmp4* (A,B, E,F) and *bmp2b* (C,D,G,H) expression in *bmp4^{st72}* mutants and wild-type siblings at bud stage (A–D) and 24 hpf (E–H). *bmp4* and *bmp2b* expression in *bmp4^{st72}* mutants (B,D) is similar to that seen in their wild-type siblings (A,C) at bud stage. At 24 hpf, a gap in the *bmp4* and *bmp2b* expression patterns is apparent in the ventral tail fin (arrowheads) in *bmp4^{st72}* mutants (F,H). However, expression in other regions is unaffected, suggesting that the absence of staining is more likely due to the lack of ventral tail fin fate than a direct effect on expression levels. A–D are lateral views with dorsal to the right; E–H are lateral views with anterior to the left.

**Figure 7.**

Model for early and late phase BMP signaling. (A–C) A gradient model of BMP function predicts expanded intermediate fates. Tail mesoderm and blood fates (TM, BL) are induced in cells at positions along the dorsoventral axis (x-axis) that are exposed to levels of BMP signaling (y-axis) between certain thresholds as indicated by dotted lines. More ventral tail fates, like cloaca and ventral tail fin, require higher BMP levels. (A) In wild-type embryos, a steep BMP gradient ensures that all cell fates are specified. (B) In embryos with compromised BMP signaling, a shallower BMP gradient forms. As a result, more cells along the dorsoventral axis receive levels of BMP signaling that fall within the upper and lower thresholds for tail mesoderm and blood, and thus these fates are expanded. This expansion comes at the expense of the more ventral cloaca (CL) and ventral tail fin (VTF) fates, which are reduced. (C) In embryos in which BMP signaling is reduced even further, very little blood and tail mesoderm develops and no cloacal or ventral tail fin fates are specified. Adapted from (Nguyen et al., 1998). (D) In the late blastula and early gastrula, BMP2b and BMP7, functioning as

heterodimers and signaling through Alk8 and Smad5, specify ventral derivatives and set aside a tail domain. During this early phase, BMP2b and BMP7 activate their own expression as well as that of *smad1* and *bmp4*. In the late phase of BMP signaling, BMP2b and BMP4 specify ventroposterior fates, acting additively as morphogens and signaling through Smad1.

Table 1Molecular characterization of *vox/vent* enhancers.

Allele	Gene/LG	Lesion	Zygotic Phenotype	Genetic Features
<i>st30</i>	<i>smad5</i>	N(315)L	C1–C4	Dominant maternal effect (C1–C4)
<i>st31</i>	<i>smad5</i>	W(434)R	C2	Partially penetrant maternal-zygotic effect (75% C1)
<i>st32</i>	<i>smad5</i>	R(91)C	C1	Homozygous viable; recessive maternal effect (100% C3/C4)
<i>st33</i>	LG14 near <i>smad5</i>	?	C1	Homozygous viable; recessive maternal effect (100% C1–C4)
<i>st37</i>	<i>bmp4</i>	insertion in 5'UTR	C1	Homozygous viable; no maternal effect

Table 2

TA-cloning of RT-PCR from *bmp4*^{st37} heterozygotes.

Female Genotype	Male Genotype	Stage	F primer	R primer	# Mutant clones	# WT clones
+/+	st37/st37	50% epiboly	E1F	E4R	0	37 (100%)
+/+	st37/st37	24hpf	E1F	E4R	1	33 (97%)
+/+	st37/st37	50% epiboly	E3F	E4R	2	76 (97%)
+/+	st37/st37	24hpf	E3F	E4R	3	73 (96%)
st37/st37	+/+	70% epiboly	E1F	E4R	1	28 (97%)
st37/st37	+/+	24hpf	E1F	E4R	0	32 (100%)
st37/st37	+/+	70% epiboly	E3F	E4R	1	23 (96%)
st37/st37	+/+	24hpf	E3F	E4R	1	31 (97%)
st37/+	—	Adult ovary	E3F	E4R	11	18(62%)
st37/+	—	Adult ovary	E1F	E4R	2	92 (98%)

Table 3

Genetic interactions between *sw^{fa72}*, *bmp4^{st72}*, *snh^{ty68a}*.

Genotype	C2	C1B	C1S	C1W	WT
<i>sw^{fa72}/+; bmp4^{st72}/bmp4^{st72}; snh^{ty68a}/+</i>	32 (100%)				
<i>sw^{fa72}/+; bmp4^{st72}/bmp4^{st72}</i>	15 (44%)	10 (29%)	7 (21%)	2 (6%)	
<i>sw^{fa72}/+; bmp4^{st72}/+; snh^{ty68a}/+</i>	18 (42%)	9 (21%)	16 (37%)		
<i>sw^{fa72}/+; bmp4^{st72}/+</i>			30 (68%)	13 (30%)	1 (2%)
<i>sw^{fa72}/+; snh^{ty68a}/+</i>			12 (46%)	12 (46%)	2 (8%)
<i>bmp4^{st72}/bmp4^{st72}; snh^{ty68a}/+</i>			8 (28%)	21 (72%)	
<i>bmp4^{st72}/bmp4^{st72}</i>			2 (9%)	14 (64%)	6 (27%)
<i>bmp4^{st72}/+; snh^{ty68a}/+</i>			2 (5%)	17 (40%)	23 (55%)
<i>sw^{fa72}/+</i>			1 (4%)	9 (36%)	15 (60%)
<i>snh^{ty68a}/+</i>				1 (3%)	34 (97%)
<i>bmp4^{st72}/+</i>					43 (100%)
wildtype					31 (100%)

Embryos were obtained from multiple crosses between a single *sw^{fa72}*, *bmp4^{st72}*, *snh^{ty68a}* heterozygous female and a *bmp4^{st72}* heterozygous male.